

Activated aging dynamics and negative fluctuation-dissipation ratios

Peter Mayer,^{1,2} Sébastien Léonard,³ Ludovic Berthier,³ Juan P. Garrahan,⁴ and Peter Sollich²

¹*Department of Chemistry, Columbia University, 3000 Broadway, New York, NY 10027, USA*

²*King's College London, Department of Mathematics, London WC2R 2LS, U.K.*

³*Laboratoire des Colloïdes, Verres et Nanomatériaux UMR 5587,*

Université Montpellier II and CNRS, 34095 Montpellier Cedex 5, France

⁴*School of Physics and Astronomy, University of Nottingham, Nottingham, NG7 2RD, UK*

(Dated: February 8, 2020)

In glassy materials aging proceeds at large times via thermal activation. We show that this can lead to negative dynamical response functions and novel and well-defined violations of the fluctuation-dissipation theorem, in particular, negative fluctuation-dissipation ratios. Our analysis is based on detailed theoretical and numerical results for the activated aging regime of simple kinetically constrained models. The results are relevant to a variety of physical situations such as aging in glass-formers, thermally activated domain growth and granular compaction.

PACS numbers: 05.70.Ln, 75.40.Gb, 05.40.-a, 75.40.Mg

Glassy materials display increasingly slow dynamics when approaching their amorphous state. At the glass transition, where relaxation times exceed experimentally accessible timescales, they change from equilibrated fluids to non-equilibrium amorphous solids. In the glassy phase, physical properties are not stationary and the system ages [1]. A full understanding of the non-equilibrium glassy state remains a central theoretical challenge.

An important step forward was the mean-field description of aging dynamics for both structural and spin glasses [2]. In this context, thermal equilibrium is never reached and aging proceeds by downhill motion in an increasingly flat free energy landscape [3]. Two-time correlation and response functions depend explicitly on both their arguments, and while the fluctuation-dissipation theorem (FDT) does not hold it can be generalized using the concept of a fluctuation-dissipation ratio (FDR). This led in turn to the idea of effective temperatures [4], and a possible thermodynamic interpretation of aging [2, 5].

While some experiments and simulations [6] appear to confirm the existence of a mean-field aging regime, in many systems of physical interest, such as liquids quenched below the glass transition or domain growth in disordered magnets, the dynamics is not of mean-field type, displaying both activated processes and spatial heterogeneity [7, 8]. The nature of FDT violations in such systems is unclear. Theoretical studies have found ill-defined FDRs [9], non-monotonic response functions [10, 11, 12, 13], observable dependence [14, 15], non-trivial FDRs in the absence of thermodynamic transitions [16] and a subtle interplay between growing dynamical correlation lengthscales and FDT violations [17, 18]. Experiments have in addition detected anomalously large FDT violations associated with intermittent dynamics [19].

Here, we study kinetically constrained models [20], which are simple models for generic glassy systems with heterogeneous dynamics and dynamical lengthscales that diverge as temperature is lowered. In these systems aging proceeds at large times through thermal activation. We

show that FDT violations in the activated regime retain a simple structure with well-defined FDRs, elucidate the physical origin of negative dynamical response functions, and predict the existence of negative FDRs for observables that are directly coupled to activated processes.

We focus mainly on the one-spin facilitated model of Fredrickson and Andersen [21] (FA model), defined in terms of a binary mobility field, $n_i \in \{0, 1\}$, on a cubic lattice; $n_i = 1$ indicates that a site is excited (or mobile). The system evolves through single-site dynamics obeying detailed balance with respect to the energy function $H = \sum_i n_i$. The dynamics is subject to a kinetic constraint such that changes at site i are permitted only if at least one nearest neighbour of i is in its excited state. In any spatial dimension d , relaxation times follow an Arrhenius law at low temperatures [20, 22].

At low temperatures, $T < 1$, the dynamics of the FA model is effectively that of diffusing excitations, which can coalesce and branch [22, 23]. Such a problem can be described in the continuum limit by a dynamical field theory action with complex fields $\varphi(\mathbf{r}, t)$, $\bar{\varphi}(\mathbf{r}, t)$ [22, 24],

$$S = \int_{\mathbf{r}, t} \bar{\varphi}(\partial_t - D\nabla^2 - \gamma)\varphi - \gamma\bar{\varphi}^2\varphi + \lambda\bar{\varphi}(1 + \bar{\varphi})\varphi^2, \quad (1)$$

with $n_i \rightarrow (1 + \bar{\varphi})\varphi$ [24]. In terms of the equilibrium concentration of excitations, $c \equiv \langle n_i \rangle = 1/(1 + e^{1/T})$, the effective rates for diffusion, coalescence and branching are, respectively, $D \propto c$, $\lambda \propto c$, and $\gamma \propto c^2$ [22, 23]. The aging dynamics following a quench from $T = \infty$ to low T consists of two regimes. Initially, clusters of excitations coalesce on timescales of $O(1)$, reaching a state made of isolated excitations. This process and the subsequent energy plateau are reminiscent of the descent to the threshold energy in mean-field models [2]. For times larger than $1/D$, excitations diffuse via thermal activation and decrease the energy as they coalesce.

Following [25] we calculated the connected two-time

correlation to all orders in λ at tree level,

$$\begin{aligned} N C_q(t, t_w) &= \langle \varphi_q(t) \varphi_{-q}(t_w) \rangle + \langle \varphi_q(t) \bar{\varphi}_{-q}(t_w) \rangle \langle \varphi_0(t_w) \rangle \\ &\approx N t_w (\lambda t^2)^{-1} e^{-Dq^2(t-t_w)} f(z). \end{aligned}$$

Here $C_q(t, t_w)$ is the Fourier transform of $\langle n_i(t) n_j(t_w) \rangle_c \equiv \langle n_i(t) n_j(t_w) \rangle - \langle n_i(t) \rangle \langle n_j(t_w) \rangle$, and $\varphi_q(t), \bar{\varphi}_q(t)$ are those of $\varphi(\mathbf{r}, t), \bar{\varphi}(\mathbf{r}, t)$. Subscripts q indicate wavevector, N is the system size, and $z \equiv Dq^2 t_w$. We have assumed that both waiting time t_w and final time t are large ($\gg 1/D$), and set $\gamma = 0$ to get the leading contribution at low T . The function $f(z)$ goes as $f \approx 1 - 1/z$ for $z \gg 1$, and $f \approx (1+z)/3$ for $z \ll 1$. At $q = 0$ we get the energy auto-correlation: $C_0(t, t_w) = N^{-1} \langle H(t) H(t_w) \rangle_c \approx n(t) t_w / (3t)$, where $n(t) = \langle n_i(t) \rangle \approx (\lambda t)^{-1}$ is the mean energy per site. These classical expressions should be accurate above the critical dimension d_c where fluctuations are negligible. The limit $\gamma = 0$ corresponds to diffusion limited pair coalescence (DLPC) which has $d_c = 2$ [24].

Consider now a perturbation $\delta H = -h_q A_q$ at time t_w , with $A_q = \sum_i \cos(\mathbf{q} \cdot \mathbf{r}_i) n_i$. The action changes by [26]

$$T \frac{\delta S}{\delta h_q} = \int_{p,s} \lambda \bar{\varphi}_p \varphi_s \varphi_{-q-p-s} + \int_p D \bar{\varphi}_p \varphi_{-q-p} p(p+2q),$$

to leading order in c . For the two-time response function $N R_q(t, t_w) = T \delta \langle A_q(t) \rangle / \delta h_q(t_w) = -T \langle \varphi_{-q}(t) \frac{\delta S}{\delta h_q}(t_w) \rangle$ we then find at tree level

$$R_q(t, t_w) \approx (\lambda t^2)^{-1} e^{-Dq^2(t-t_w)} (z - 1). \quad (2)$$

The energy response follows as $R_0(t, t_w) \approx -n(t)/t$. The corresponding susceptibility, $\chi_0(t, t_w) = \int_{t_w}^t dt' R_0(t, t')$ is always negative, and proportional to the density of excitations at time t , $\chi_0(t, t_w) \approx -n(t)(1 - t_w/t)$.

The FDR $X_q(t, t_w)$, defined through $R_q(t, t_w) = X_q(t, t_w) \partial_{t_w} C_q(t, t_w)$ if T is included in R_q , reads

$$X_q(t, t_w) \approx \frac{z - 1}{(1 + \partial_z) z f(z)} \approx \begin{cases} 1 - 1/z & (z \gg 1) \\ -3 + 12z & (z \ll 1) \end{cases}.$$

At any waiting time t_w , for inverse wavevectors q^{-1} smaller than the dynamical correlation length, $\xi(t_w) = \sqrt{D t_w}$, FDT is recovered: $X_q \approx 1$. However, at small wavevectors, $q \xi \ll 1$, the FDR becomes negative. In the $q \rightarrow 0$ limit, one gets the FDR for energy fluctuations,

$$X_\infty \equiv X_0(t, t_w) = -3 \quad (d > d_c). \quad (3)$$

FDT violations thus take a particularly simple form reminiscent of the one found in non-equilibrium critical dynamics [15]. On large, non-equilibrated lengthscales a quasi-FDT holds with T replaced by an “effective temperature”, T/X_∞ . Contrary to pure ferromagnets, however, X_∞ is *negative*. This feature is not predicted by earlier mean-field studies as it is a direct consequence of thermal activation: if temperature is perturbed upwards during aging, the dynamics is accelerated; the energy decay is then faster, giving a negative energy response.

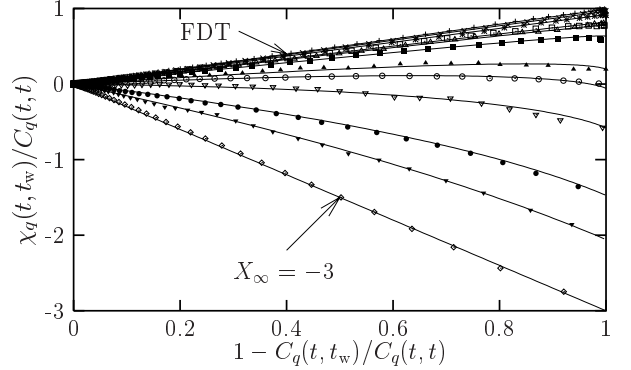


FIG. 1: Normalized FD-plots for the FA model at $T = 0.1$ in $d = 3$ with fixed $t = 2 \times 10^5$ and running $t_w \in [0, t]$. Symbols are results from simulations, full lines are the tree-level predictions. Wavevectors shown are $q = \pi/x$ with $x = 1, 2, 2.4, 3, 3.2, 4, 5.33, 6, 8, 12$, and 16 (top to bottom). System size was $N = 32^3$. Averages are over 4×10^4 initial conditions.

The fluctuation-dissipation (FD) plots in Fig. 1 show that the tree-level calculations compare very well with numerical simulations of the FA model in $d = 3$. We have also confirmed the diffusive scaling with $z = Dq^2 t_w$. Simulations were performed using continuous time Monte Carlo. We measure $C_q(t, t_w)$ as the auto-correlation of the observable A_q , on a cubic lattice with periodic boundary conditions, $N = L^3$ and a linear size $L \gg \sqrt{D t_w}$. The susceptibility $\chi_q(t, t_w)$ is obtained by direct generalization of the “no-field” method of [27] to continuous time. We show data using the prescription of Ref. [28], plotting $\chi_q(t, t_w)/C_q(t, t)$ as a function of $1 - C_q(t, t_w)/C_q(t, t)$ for fixed observation time, t , and varying waiting time, $0 < t_w \leq t$. The abscissa runs from 0 ($t_w = t$) to ≈ 1 ($t_w \ll t$). Using t_w as the running variable ensures that the slope of the plot is, by definition, the FDR $X_q(t, t_w)$ [15]. Other procedures, e.g. keeping t_w fixed, would give very different results [9, 10, 11, 12, 13] that could lead to erroneous conclusions.

In dimensions $d < d_c$ we need to take fluctuations into account. For $d = 1$ exact scaling results can be derived for the FA model by considering a DLPC process with diffusion rate $D = c/2$. Because the long-time behaviour of DLPC dynamics is diffusion controlled [24] we are free to choose the coalescence rate as $\lambda = D$ without affecting scaling results in the long-time regime ($t, t_w \gg 1/c$) [29]. We focus on the low temperature dynamics ($c \rightarrow 0$) and times $t \ll 1/\gamma \propto 1/c^2$ where branching can be neglected; the system is then still far from equilibrium as it ages.

To analyse our DLPC process we use the standard quantum mechanical formalism [30]: probabilities are mapped to states $|P(t)\rangle = \sum_{\mathbf{n}} p(\mathbf{n}, t) |\mathbf{n}\rangle$, where $|\mathbf{n}\rangle = |n_1, \dots, n_N\rangle$, so that the master equation reads $\partial_t |P(t)\rangle = W_C |P(t)\rangle$, with W_C the DLPC master operator. Correlations are then $\langle A(t) A(t_w) \rangle = \langle 1 | A e^{W_C \Delta t} A e^{W_C t_w} | P(0) \rangle$, where $\langle 1 | = \sum_{\mathbf{n}} \langle \mathbf{n} |$ and $\Delta t \equiv t - t_w$. DLPC dynamics is closely related to diffu-

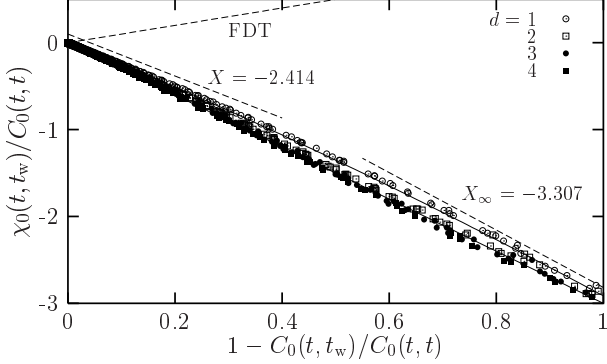


FIG. 2: Normalized energy FD-plots for the FA model in dimensions $d = 1$ to 4, for fixed times t and running waiting times $t_w \in [0, t]$. For each d we show simulation data (symbols) for several parameters [32]. Full curves show a straight line with slope $X_\infty = -3$ and the exact limit plot in $d = 1$ with asymptotic slopes shown as dashed lines.

sion limited pair-annihilation (DLPA) [30] by a similarity transformation B : $W_C = BW_AB^{-1}$ where W_A is the DLPA master operator with diffusion rate $D = c/2$ and annihilation rate $2\lambda = c$. Introducing empty and parity interval observables, $E_i = \prod_{k=i_1}^{i_2-1} (1 - n_k)$ and $P_i = \prod_{k=i_1}^{i_2-1} (1 - 2n_k)$ respectively, where $i = (i_1, i_2)$, one has $\langle 1 | E_i e^{W_C \Delta t} = \langle 1 | P_i e^{W_A \Delta t} B^{-1}$, $\langle 1 | B = \langle 1 |$ and $\langle 1 | n_i B = 2\langle 1 | n_i$ [30]. If we interpret the n_i in DLPA as domain walls in an Ising spin system, $n_i = \frac{1}{2}(1 - \sigma_i \sigma_{i+1})$, then $P_i \equiv \sigma_{i_1} \sigma_{i_2}$, and $W_A \equiv W_\sigma$ becomes the $T = 0$ master operator for the Glauber-Ising spin chain. Substituting the two-spin propagator $\langle 1 | \sigma_{i_1} \sigma_{i_2} e^{W_\sigma c \Delta t}$ derived in [31] and mapping back to DLPC then gives

$$\langle 1 | E_i e^{W_C \Delta t} = H_{i_2 - i_1}(2c \Delta t) \langle 1 | + \sum_{j_1 < j_2} G_{i,j}^{(2)}(c \Delta t) \langle 1 | E_j, \quad (4)$$

where $G_{i,j}^{(2)}(\cdot)$ and $H_n(\cdot)$ are given in [31]. As motivated above, the difference between Eq. (4) and the empty interval propagator, $\langle 1 | E_i e^{W \Delta t}$, for the true FA master operator W will be negligible in the low-temperature, long-time, far-from-equilibrium aging regime we consider.

Eq. (4) together with the identity $n_i = 1 - E_{(i,i+1)}$ is the key ingredient for the calculation of the two-time energy correlation and response functions $C_0(t, t_w), R_0(t, t_w)$ in the $d = 1$ FA model [29]. Qualitatively a picture similar to $d > d_c$ emerges, but with the FDR now showing a weak dependence on the ratio t/t_w . At equal times, $X_0(t/t_w \rightarrow 1) = -(1 + \sqrt{2}) = -2.414 \dots$, while for $t/t_w \rightarrow \infty$ the FDR approaches

$$X_\infty = \frac{3\pi}{16 - 6\pi} = -3.307 \dots \quad (d = 1). \quad (5)$$

Fig. 2 demonstrates complete agreement between our scaling predictions and simulation data in all dimensions. In $d = 1$ the data fall on the curved limit FD-plot [29]

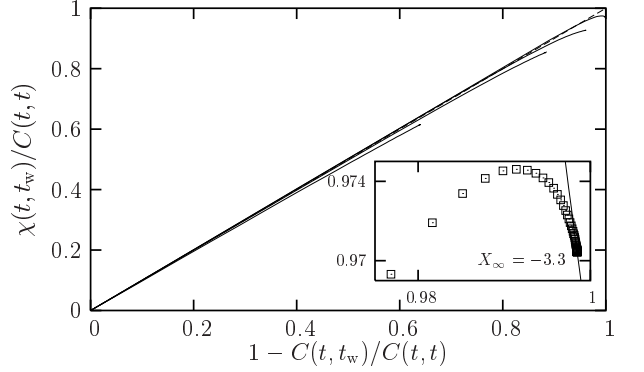


FIG. 3: Normalized FD-plot for the local observable n_i in the $d = 1$ FA model at $T = 0.1$ and $t = 2 \times 10^4, 5 \times 10^4, 10^5$ and 10^6 (bottom to top). The dashed diagonal is FDT. Inset: final part of the $t = 10^6$ data, enlarged to show the non-monotonic response and $X_\infty \approx -3.307$ (full line).

derived from (4). In dimensions $d = 3, 4$ the simulations are compatible with a constant FDR $X_\infty = -3$, Eq. (3). The data for $d = d_c = 2$ suggest a slightly curved limit plot, possibly due to logarithmic corrections, but are still compatible with $X_\infty \approx -3$.

Numerically, the no-field method of [27] becomes unreliable for small q . To get precise data as shown in Fig. 2 we used instead the exact relation

$$2R_0(t, t_w) = (1 - 2c) \partial_{t_w} n(t) + \partial_{t_w} C_0(t, t_w) + C_*(t, t_w).$$

Here $C_*(t, t_w) = N^{-1} \langle H(t) U(t_w) \rangle_c$, with $U = \sum_i f_i (n_i - c)$, and $f_i \in \{0, 1\}$ the kinetic constraint. This result is obtained as follows: $\partial_{t_w} D(t, t_w) = N^{-1} \langle 1 | H e^{W \Delta t} [H, W] | P(t_w) \rangle$, with $D(t, t_w) = N^{-1} \langle H(t) H(t_w) \rangle$ denoting the full energy correlation, and $[X, Y] \equiv XY - YX$. Similarly, $R_0(t, t_w) = N^{-1} \langle 1 | H e^{W \Delta t} V | P(t_w) \rangle$ where $V = T \partial_{h_0} W = T^2 \partial_T W$. Combining these expressions produces $2R_0 - \partial_{t_w} D = N^{-1} \langle 1 | H e^{W \Delta t} (2V - [H, W]) | P(t_w) \rangle$. One can show that $2V - [H, W] = (1 - 2c)W + U$, so that non-diagonal terms in this expression are proportional to W . Consequently, $2R_0 - \partial_{t_w} D = (1 - 2c) \partial_{t_w} n(t) + N^{-1} \langle H(t) U(t_w) \rangle$. Switching from full to connected correlators gives after some algebra the above result for $R_0(t, t_w)$, which enables very efficient no-field energy response measurements.

The auto-correlation $C(t, t_w) = \langle n_i(t) n_i(t_w) \rangle_c$, and associated auto-response, $R(t, t_w) = T \delta \langle n_i(t) \rangle / \delta h_i(t_w)$, to a local perturbation $\delta H = -h_i n_i$, also have a negative FDR regime. Previous studies [13, 16] had suggested that the corresponding FD-plot has an equilibrium form, even during aging. A more careful analysis, however, reveals nonequilibrium contributions (Fig. 3). Exact long-time predictions for $C(t, t_w)$ and $R(t, t_w)$, and the resulting FDR, can be derived from (4) [29]. One finds that, as for the energy, the FDR has the aging scaling $X(t/t_w)$. It crosses over from quasi-equilibrium behaviour, $X \approx 1$, at $t/t_w \approx 1$, to $X \approx X_\infty$ for $t/t_w \gg 1$; notably, X_∞ here is

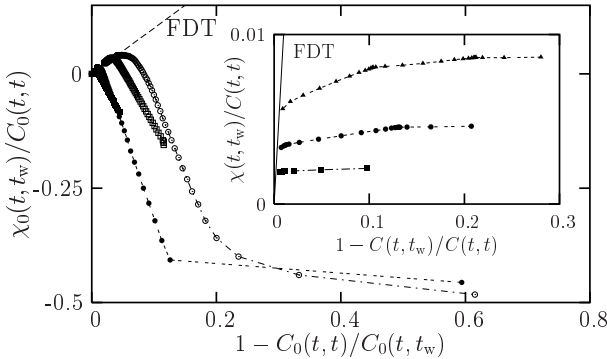


FIG. 4: Normalized energy FD-plots for the East model for $(T, t) = (.15, 100), (.15, 10^5), (.2, 50)$ and $(.2, 5000)$ (from left to right). Inset: Normalized FD-plot for local observables for $T = 0.15$ and $t = 10^2, 10^5$ and 10^7 (from bottom to top).

the *same* as for the energy, Eq. (5). However, the region in the FD-plot that reveals the nonequilibrium behaviour shrinks as $O(1/\sqrt{t})$ as t grows. This explains previous observations of pseudo-equilibrium and makes a numerical measurement of X_∞ from the local observable n_i very difficult. On the other hand, with the coherent counterpart, i.e. the energy, Fig. 2 shows that this would be straightforward, confirming a point made in [15]. Numerical simulations for $d > 1$ produce local FD-plots analogous to Fig. 3 but with $X_\infty = -3$. We emphasize that non-monotonicity of these FD-plots is not an artefact of

the parametrization with t , as in, e.g., [9, 12].

Our arguments show that negative out-of-equilibrium responses should occur generically in systems with activated dynamics for observables whose relaxation couples to these activation effects; activation need not be thermal, but can be via macroscopic driving, e.g. tapping of granular materials [10, 33]. To illustrate how quantitative effects may vary, we consider briefly the East model [20] of fragile glasses, leaving all details for a separate report. The behaviour is richer due to the hierarchical nature of the relaxation, which leads to plateaux in the energy decay. Properly normalized energy FD-plots nevertheless have a simple structure, with three regimes (Fig. 4): for given t , equilibrium FDT is obeyed at small time differences $t - t_w$, indicating quasi-equilibration within a plateau; a regime with a single negative FDR follows, coming from the activated relaxation process preceding the plateau at t ; finally, the plot becomes horizontal, corresponding to all previous relaxation stages which decorrelate the system but do not contribute to the energy response. Interestingly, in the FD-plots for auto-correlation and auto-response (Fig. 4, inset), each relaxation stage of the hierarchy is associated with a well-defined effective temperature, a structure reminiscent of that found in mean-field spin glasses [2].

This work was supported by the Austrian Academy of Sciences and EPSRC grant 00800822 (PM); EPSRC grants GR/R83712/01, GR/S54074/01, and University of Nottingham grant FEF3024 (JPG).

[1] *Spin Glasses and Random Fields*, edited by A.P. Young (World Scientific, Singapore, 1998).

[2] L.F. Cugliandolo and J. Kurchan, Phys. Rev. Lett. **71**, 173 (1993); J. Phys. A **27**, 5749 (1994).

[3] J. Kurchan and L. Laloux, J. Phys. A **29**, 1929 (1996).

[4] L. F. Cugliandolo, J. Kurchan, and L. Peliti, Phys. Rev. E **55**, 3898 (1997).

[5] S. Franz, M. Mézard, G. Parisi, and L. Peliti, Phys. Rev. Lett. **81**, 1758 (1998).

[6] A. Crisanti and F. Ritort, J. Phys. A **36**, R181 (2003).

[7] D.S. Fisher and D.A. Huse, Phys. Rev. Lett. **56**, 1601 (1986).

[8] M.D. Ediger, Annu. Rev. Phys. Chem. **51**, 99 (2000).

[9] A. Crisanti, F. Ritort, A. Rocco, and M. Sellitto, J. Chem. Phys. **113**, 10615 (2000); P. Viot, J. Talbot, and G. Tarjus, Fractals **11**, 185 (2003).

[10] M. Nicodemi, Phys. Rev. Lett. **82**, 3734 (1999).

[11] J.P. Garrahan and M.E.J. Newman, Phys. Rev. E **62**, 7670 (2000).

[12] F. Krzakala, Phys. Rev. Lett. **94**, 077204 (2005).

[13] A. Buhot, J. Phys. A **36**, 12367 (2003).

[14] S. Fielding and P. Sollich, Phys. Rev. Lett. **88**, 050603 (2002).

[15] P. Mayer, L. Berthier, J.P. Garrahan, and P. Sollich, Phys. Rev. E **68**, 016116 (2003); **70**, 018102 (2004).

[16] A. Buhot and J.P. Garrahan, Phys. Rev. Lett. **88**, 225702 (2002).

[17] A. Barrat and L. Berthier, Phys. Rev. Lett. **87**, 087204 (2001).

[18] H.E. Castillo, C. Chamon, L.F. Cugliandolo, and M.P. Kennett, Phys. Rev. Lett. **88**, 237201 (2002).

[19] L. Bellon, S. Ciliberto and C. Laroche, Europhys. Lett. **53**, 511 (2001).

[20] F. Ritort and P. Sollich, Adv. Phys. **52**, 219 (2003).

[21] G.H. Fredrickson and H.C. Andersen, Phys. Rev. Lett. **53**, 1244 (1984).

[22] S. Whitelam, L. Berthier, and J.P. Garrahan, Phys. Rev. Lett. **92**, 185705 (2004); Phys. Rev. E **71**, 026128 (2005).

[23] M. Schulz and S. Trimper, J. Stat. Phys. **94**, 173 (1999).

[24] For a recent review see U.C. Täuber, M. Howard, and B.P. Vollmayr-Lee, J. Phys. A **38**, R79 (1999).

[25] B.P. Lee, J. Phys. A **27**, 2633 (1994).

[26] The form of the diffusion term arises because hopping is via creation of a defect at the arrival site. The hopping rate from site j to i depends only on the field at site i .

[27] C. Chatelain, J. Stat. Mech. P06006 (2004).

[28] P. Sollich, S. Fielding, and P. Mayer, J. Phys. Condens. Matter **14**, 1683 (2002).

[29] P. Mayer and P. Sollich, unpublished.

[30] K. Krebs, M.P. Pfannmüller, B. Wehefritz, H. Hinrichsen, J. Stat. Phys. **78**, 1429 (1995).

[31] P. Mayer and P. Sollich, J. Phys. A **37**, 9 (2004).

[32] Parameter values (T, t) for $d = 1$ were: $(.2, 10^5), (.1, 10^6), (.08, 10^7), (.08, 5 \times 10^7), (.08, 10^8), (.07, 10^8)$. For $d = 2$:

$(.1, 10^6), (.08, 10^6), (.08, 2 \times 10^6), (.08, 5 \times 10^6), (.08, 10^7), (.07, 10^7), (.07, 5 \times 10^7), (.06, 10^8), (.06, 5 \times 10^8)$. For $d = 3$: $(.12, 2 \times 10^4), (.1, 2 \times 10^5), (.08, 10^6), (.08, 2 \times 10^6), (.08, 5 \times 10^6), (.07, 10^7), (.06, 10^8)$. For $d = 4$: $(.1, 2 \times 10^5),$

$(.08, 10^6), (.08, 5 \times 10^6), (.07, 10^7), (.06, 10^8)$.
[33] M. Depken and R. Stinchcombe, Phys. Rev. E **71**, 065102 (2005).